

To Mix or To Merge: Toward Multi-Domain Reinforcement Learning for Large Language Models

Haoqing Wang^{1†}, Xiang Long^{1†}, Ziheng Li^{2,1†}, Yilong Xu¹, Tingguang Li¹,
and Yehui Tang¹ ✉

¹ Samsung Research, Beijing, China ² Peking University
{haoqing.wang, yehui.tang}@samsung.com

[†] Equal Contribution ✉ Corresponding Author

Abstract

Reinforcement Learning with Verifiable Rewards (RLVR) plays a key role in stimulating the explicit reasoning capability of Large Language Models (LLMs). We can achieve expert-level performance in some specific domains via RLVR, such as coding or math. When a general multi-domain expert-level model is required, we need to carefully consider the collaboration of RLVR across different domains. The current state-of-the-art models mainly employ two different training paradigms for multi-domain RLVR: mixed multi-task RLVR and separate RLVR followed by model merging. However, most of the works did not provide a detailed comparison and analysis about these paradigms. To this end, we choose multiple commonly used high-level tasks (e.g., math, coding, science, instruction following, and agent) as our target domains and design extensive qualitative and quantitative experiments using open-source datasets. We find the RLVR across domains exhibits few mutual interferences, and reasoning-intensive domains demonstrate mutually synergistic effects. Furthermore, we analyze the internal mechanisms of mutual gains from the perspectives of weight space geometry, information constraints, model prediction behavior and self-verification. This project is named as *M2RL* that means *Mixed* multi-task training or separate training followed by model *Merging* for *Reinforcement Learning*, and the homepage is at <https://github.com/Mosi-AI/M2RL>.

1 Introduction

Large language models (LLMs) (Jaech et al., 2024; Guo et al., 2025; Yang et al., 2025) have achieved significant success in various natural language processing (NLP) tasks and more challenging reasoning tasks, i.e., mathematics and software engineering. Extensive pre-training on trillion-token scale corpora is indispensable for the acquisition of comprehensive world knowledge and potential reasoning capabilities. Furthermore, the post-training process serves to stimulate explicit reasoning capabilities and align the model’s outputs with human-centric stylistic and structural expectations. During the post-training process, Reinforcement Learning with Verifiable Rewards (RLVR) (Zhang et al., 2025) plays a key role and has gained significant attention (Wen et al., 2025; Gao et al., 2025).

With the help of RLVR, many works have achieved incredibly powerful task solving abilities in some specific domains, such as coding (Zhu et al., 2024; Hui et al., 2024) and math (Yang et al., 2024; Shao et al., 2024). When we further want to obtain a general expert-level model that excels at solving tasks from different domains, the cross-domain reinforcement learning is essential. Considering that multi-task reinforcement learning may encounter gradient interference (Bai et al., 2023; Wu et al., 2025), it is important to deeply analyze the collaboration of multi-domain RLVR. The existing state-of-the-art models (Guo et al., 2025; Yang et al., 2025; Zeng et al., 2025; Xiao et al., 2026) typically apply two training paradigms: 1) mixed multi-task RLVR learns based on heterogeneous rewards from different domains simultaneously; 2) separate domain-specific reinforcement learning and then merging different expert models with weight merge (Hitit et al., 2025) or distillation (Agarwal et al.,

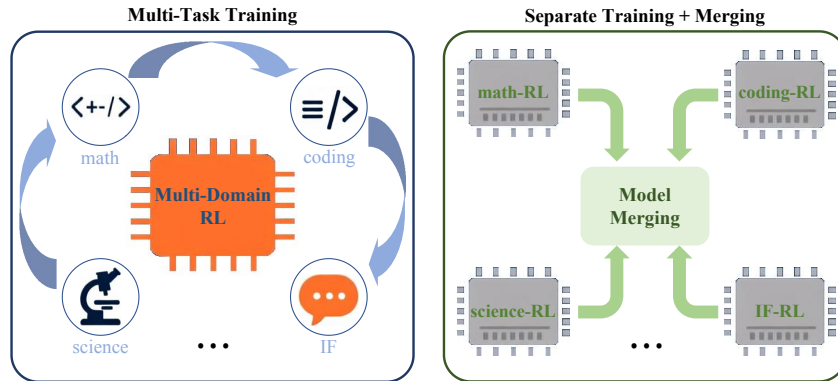


Figure 1: The two training paradigms for multi-domain RLVR: mixed multi-task training and separate training followed by model merging.

2024). However, most of these works did not share key insights about the comparison between the two training paradigms and their internal mechanisms. In this work, we aim to fill this gap by detailed comparisons and analyses.

We mainly examine five common RLVR domains: math, coding, science, instruction following, and agent. The Qwen3-4B-Base model (Yang et al., 2025) is used as the initial model of post-training for both reliability and operability. We use the open-source datasets from Nemotron 3 Nano (Blakeman et al., 2025) for both supervised fine-tuning and reinforcement learning in different domains. The final training datasets follow the data blend proportion in their technical report. When we obtain multiple domain-specific expert models, we consider both the weight merging methods (i.e., average merging (Wortsman et al., 2022), task arithmetic merging (Ilharco et al., 2022), Ties-merging (Yadav et al., 2023b) and SCE (Wan et al., 2025)) and multi-teacher on-policy distillation (Agarwal et al., 2024) for merging them. The framework illustrate of these two training paradigms are shown in Figure 1.

We compare the obtained models at multiple benchmarks across these five domains using Avg@K metric, and analyze the internal mechanisms from the perspectives of weight space geometry, information constraints, model prediction behavior and self-verification. The main findings are as follows:

- The mixed multi-task RLVR can achieve comparable performance with the separate RLVR followed by model merging with 63.7% GPU hours. The cross-domain RLVR manifests little inter-task interference, particularly between the reasoning-intensive domains, where the synergistic effects are observed.
- The weight shift footprints of the RLVR in different domains have significant overlap, and the cosine similarity after orthogonal random projection shows a positive correlation between different domains.
- We employ KL divergence as a metric to investigate mechanism behind multi-domain fusion methods. We observe that the neighborhood policy transfer during multi-task RLVR or model merging shapes the domain policies toward the optimal policy, thereby enhancing the performance.
- Weight merging primarily inherits the original capabilities of the single-task models, whereas the capabilities learned through multi-task training and on-policy distillation exhibit a larger divergence from those learned via single-task training.
- RLVR induces an emergent self-discrimination capability that is highly sensitive to task structures and training paradigms: while agentic, multi-turn interactions serve as a catalyst for robust process-level verification, extended multi-task RL tends to favor outcome-based accuracy at the expense of process-level rigor. It is a trade-off that can be mitigated through decoupled expert integration.

Table 1: Our SFT dataset blend strategy. The blend proportion mainly follows the Nemotron 3 Nano technical report. To this end, we conduct random sampling for the large source datasets and repeat the small ones.

Types	#Samples	Proportion (%)	Source Datasets	Sampling method
Math Formal Proofs	335,122	2.37	Nemotron-Math-Proofs-v1	random sampling
Math	2,950,525	20.89	Nemotron-Math-v2	random sampling
Science	2,263,340	16.04	Nemotron-Science-v1	repeat 10 times
Code	3,927,984	27.81	Nemotron-Competitive-Programming-v1	use all
Chat	4,309,780	30.52	Nemotron-Instruction-Following-Chat-v1	repeat 10 times
Conversational Agent	335,122	2.37	Nemotron-Agentive-v1	use all
Total	14121873	100.00	-	-

2 Related Works

2.1 Reinforcement Learning with Verifiable Rewards

The introduction of DeepSeek-R1 (Guo et al., 2025) has brought a widespread and rapid expansion of research into the Reinforcement Learning with Verifiable Rewards (RLVR) paradigm (Zhang et al., 2025). These works have been comprehensive and explored numerous critical aspects of implementation, such as reward design (Albalak et al., 2025; Chen et al., 2025; Lambert et al., 2024), policy optimization (Shao et al., 2024; Zheng et al., 2025; Yu et al., 2025), sampling strategy (Cui et al., 2025; Dong et al., 2025) and various insightful observations (Yue et al., 2025).

Recent studies have utilized RLVR to achieve expert-level performance in some specific domains, such as coding (Zhu et al., 2024; Hui et al., 2024) and math (Yang et al., 2024; Shao et al., 2024). However, the fusion of these disparate reinforcement learning domains into a general expert-level model remains an open question. DeepSeek-R1 (Guo et al., 2025) and Qwen3 (Yang et al., 2025) conduct the mixed multi-task reinforcement learning that learns different domains simultaneously. GLM-4.5 (Zeng et al., 2025) and MiMo-V2-Flash (Xiao et al., 2026) conduct the separate domain-specific reinforcement learning and then merge models with weight merging (Wan et al., 2025; Yadav et al., 2023b) or distillation (Agarwal et al., 2024). However, these representative works do not provide more insights and in-depth analysis about multi-domain RLVR. In this work, we aim to conduct extensive comparison and internal analysis about these two paradigms.

2.2 Model Merging

There are basically two methodologies for merging multiple domain-specific large language models to a general model which can achieve comparable performance in different domains with the specific model: 1) training-free weight merging (Yu et al., 2024) and 2) on/off-policy distillation. By directly blending weights, weight merging achieves functional integration without the high overhead of further training. Beyond the naive average merging, fisher merging (Matena & Raffel, 2022) calculates the fusion weights using the Fisher information matrix; TIES-Merging (Yadav et al., 2023a) resolves task conflicts via pruning, sign agreement and a final disjoint fusion of consistent signs. Besides, we can also distillation the initial model from the multiple domain-specific models. Off-policy distillation conducts supervised fine-tuning using the rollout trajectories generated by multiple domain models. Multi-teacher on-policy distillation (Agarwal et al., 2024) minimizes the Kullback-Leibler divergence between the prediction probability of the student and teacher model on the rollout trajectories, which are generated by the student model.

3 Experiments and Analysis

3.1 Preliminary

Pre-training via next-token prediction equips models with extensive world knowledge, while post-training is the process of learning how to use that knowledge to be a helpful assistant. The post-training phase typically encapsulates multiple stages and mainly contains

Table 2: Training settings and total GPU hours for different RLVR and on-policy distillation training. “IF” denotes instruction following and “MT-OPD” denotes multi-teacher on-policy distillation.

Methods	batch size	#rollout	#step	GPU Hours
Math	128	16	400	4782.3
Coding	128	16	400	6404.4
Science	128	16	400	1140.8
IF	128	16	400	1180.0
Agent	128	16	400	2271.0
Multi-Task	128	16	1000	10050.6
MT-OPD	256	4	200	967.9

Supervised Fine-Tuning (SFT) and Reinforcement Learning (RL) (Guo et al., 2025; Yang et al., 2025). During the supervised fine-tuning stage, the models are adapted to high-quality, instruction-based datasets to develop basic conversational and task-solving capabilities. During the reinforcement learning stage, the models are optimized based on the reward of their on-policy generated responses.

Instead of the reward signals that align with human preferences, the verifiable rewards provide deterministic, gold-standard feedback that eliminates reward hacking and subjective bias. Concretely, we define π_θ as the parameterized LLM policy model that generate the response \mathbf{y} to the prompt \mathbf{q} . To optimize the model performance, we employ a deterministic rewarder $R(\mathbf{q}, \mathbf{y})$ to yield a binary reward $r \in \{0, 1\}$, which strictly reflects the objective correctness of the final output. Additionally, the formatting reward is also integrated to incentivize the structural segregation of the chain-of-thought (CoT) reasoning from the terminal answer. Finally, we optimize the policy model π_θ to maximize the expected reward. In this work, we apply the representative Group Relative Policy Optimization (GRPO) (Shao et al., 2024) as our reinforcement learning algorithm.

Multi-domain reinforcement learning is an important topic in the community and its complexity stems from the potential interference between different domains. The existing state-of-the-art models (Guo et al., 2025; Yang et al., 2025; Xiao et al., 2026; Zeng et al., 2025) typically apply two different training paradigms: mixed multi-task reinforcement learning and separate reinforcement learning followed by model merging. However, they do not provide much detailed analysis and comparison. In this work, we aim to explore the best ways to combine multi-domain reinforcement learning, and provide detailed comparisons and in-depth analysis to fill the gaps. The following subsections are organized as follows: we first introduce the experimental framework and core results, subsequently diving into a detailed analysis of the underlying mechanisms from multiple perspectives.

3.2 Experimental Design and Results

Although the post-training process in existing works typically involves multiple alternating stages of SFT and RL, we adopt a simplified SFT then RL pipeline for controllable experiments. We mainly focus on five common domains: math, coding, science, instruction following and agent, which contain the complex reasoning, alignment and tool use. We apply the widely-used Qwen3-4B-Base (Yang et al., 2025) model as the starting point for supervised fine-tuning to balance both credibility and operability.

Dataset blend. We use the open-source SFT datasets¹ from Nemotron 3 Nano (Blakeman et al., 2025). We filter out the data without messages field and blend the datasets from different domains. To approximately follow the proportion of samples across different domains in the technical report, we repeat the small datasets and randomly sample from the large ones. The final SFT dataset blend strategy is shown in Table 1 and we obtain

¹<https://huggingface.co/collections/nvidia/nemotron-post-training-v3>

Table 3: The evaluation scores on 9 benchmarks across 5 different domains. The highest and second-best scores are shown in bold and underlined respectively. The results with the best model merging method are provided here.

Benchmarks	Qwen3-4B-Base	SFT	RL-Math	RL-Coding	RL-Science	RL-IF	RL-Agent	Merging	RL-Multi
<i>Math Tasks</i>									
AIME'24	9.65	56.04	77.66	61.61	64.69	67.81	57.60	<u>81.15</u>	81.20
AIME'25	5.68	51.30	70.42	55.16	56.35	60.52	54.64	74.74	<u>73.39</u>
<i>Coding Tasks</i>									
LCB v5	16.50	55.92	59.59	65.00	57.66	60.80	62.95	60.84	<u>63.21</u>
LCB v6	18.29	52.00	54.57	58.86	53.14	53.14	54.29	<u>57.71</u>	56.57
<i>Science Tasks</i>									
HLE	4.45	5.75	6.39	5.92	6.26	7.04	5.98	7.92	<u>7.18</u>
GPQA-Diamond	20.08	42.68	58.46	46.59	53.79	49.62	46.09	<u>57.58</u>	53.62
<i>Instruction Following Tasks</i>									
IFEval _{strict prompt}	35.12	79.48	80.59	78.74	78.93	90.94	81.33	<u>92.61</u>	93.53
IFBench	11.90	38.44	40.14	39.46	40.14	<u>59.52</u>	40.82	54.76	61.22
<i>Agent Tasks</i>									
BFCL v3	29.73	50.05	50.32	50.64	49.56	50.55	59.14	61.73	<u>60.74</u>

Table 4: Comparison among different model merging methods and the best result is in bold. "TA" denotes task arithmetic merging and "MT-OPD" denotes multi-teacher on-policy distillation. "LCB" denotes LiveCodeBench and "GPQA-D" denotes GPQA-Diamond.

Methods	AIME'24	AIME'25	LCB v5	LCB v6	HLE	GPQA-D	IFEval _{strict prompt}	IFBench	BFCL v3	Avg.
Average	67.55	64.38	58.92	57.71	6.16	50.13	84.84	40.82	53.17	53.74
SCE	80.73	74.84	62.01	56.57	7.28	56.57	93.35	53.74	61.19	60.70
Ties	81.15	74.74	60.84	57.71	7.92	57.58	92.61	54.76	61.73	61.00
Ties+DARE	79.84	75.89	60.71	57.71	7.41	57.07	90.94	56.12	61.05	60.75
TA	80.47	76.61	57.97	52.57	6.39	54.04	93.16	61.56	59.25	60.22
TA+DARE	81.09	76.18	58.65	56.00	6.39	55.56	93.72	62.59	58.76	60.99
MT-OPD	80.52	74.53	63.26	57.14	7.37	53.66	90.20	56.46	60.98	60.46

about 14M total samples for SFT. For RLVR, we also use the open-source RLVR datasets² from Nemotron-3 Nano, and extract the following subsets corresponding to our domains of interest: (1) *Math*: 22,056 samples from DAPO (Yu et al., 2025) and Skyworks (He et al., 2025a;b); (2) *Coding*: 19,169 samples from CodeContests (Li et al., 2022) and OpenR1 (Penedo et al., 2025); (3) *Science*: 19,670 samples from OpenScienceReasoning-2 (NVIDIA Corporation, 2025); (4) *Instruction Following*: 16,575 samples from WildChat-1M (Zhao et al., 2024) with instructions from Open-Instruct (Lambert et al., 2024); (5) *Agent*: 10,229 samples from Nemotron-RL-agent-workplace-assistant (Blakeman et al., 2025). The reinforcement learning for a single domain is conducted on the corresponding dataset, and the multi-task reinforcement learning applies the directly mixed of these datasets.

Training. For SFT, we fine-tune the initial model using 14M samples for one epoch. For reinforcement learning, the important training settings and GPU hours are provided in Table 2. Note that, due to the differences in response length and reward calculation cost, the GPU hours of each training step are different among these different domains. More details about reward design and training settings are provided in appendix A.

Model Merging. After we obtain the reinforcement-learned models from five different domains, we need to merge them to obtain a unified model. One direct paradigm is weight merging, which merges the parameters of different models with the same structure. The representative methods include average merging (Wortsman et al., 2022), task arithmetic merging (Ilharco et al., 2022), Ties-merging (Yadav et al., 2023b) and SCE (Wan et al., 2025). Moreover, we can also combine these merging methods with DARE (Yu et al., 2024), which suggests setting most delta parameters to zero before weight merging. Here we use the supervised fine-tuned model as the anchor model and set the mask ratio as 0.8 for DARE. Besides, another model merging paradigm is using multi-teacher on-policy distillation.

²<https://huggingface.co/datasets/nvidia/Nemotron-3-Nano-RL-Training-Blend>

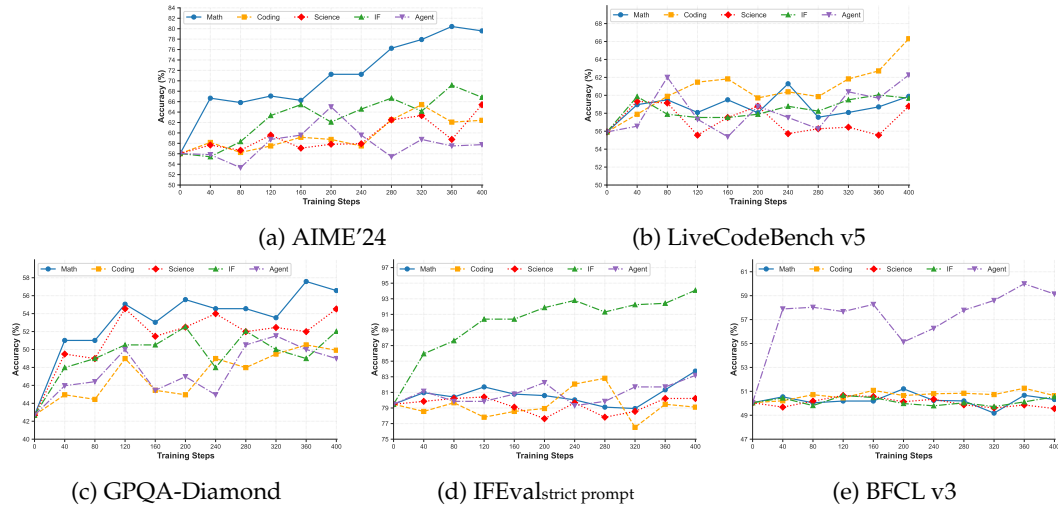


Figure 2: The accuracy change trajectory of different benchmarks during math, coding, science, instruction following and agent RLVR process.

Concretely, we use the supervised fine-tuned model as the student model and distill it from the routed teachers in five domains. The training dataset is the same as the multi-task reinforcement learning. The important training settings and GPU hours are also provided in Table 2, and more training settings are provided in appendix A.

Evaluation Results. The evaluation datasets include 9 benchmarks: AIME'24 (MAA, 2024) and AIME'25 (AIME, 2025) for math tasks, LiveCodeBench v5 and v6 (Jain et al., 2024) for coding tasks, HLE (Phan et al., 2024) for coding tasks, GPQA-Diamond (Rein et al., 2025) and GPQA-Easy (Rein et al., 2024) for science tasks, IFEval (Zhou et al., 2023) and IFBench (Pyatkin et al., 2025) for instruction following tasks, and BFCL v3 (Yan et al., 2024) for agent tasks.

The results are provided in table 3, where the best result is in bold and the second one is underlined>. Firstly, regarding the five distinct RLVR models, the models of math, coding, instruction following and agent domains all achieve the state-of-the-art performance within its respective domain tasks. The RLVR model of math domain obtains better performance than that of science domain at science tasks, and the reason maybe these two science benchmarks require more logical reasoning and numerical calculations than science knowledge. Secondly, the mixed multi-task RLVR can achieve comparable performance with separate RLVR followed by model merging with significantly less GPU hours, i.e., 63.7%. The gradient interference (Yu et al., 2020; Wu et al., 2025) among different domains is not significant, and they even have mutual benefits. Concretely, the three reasoning domains (i.e., math, coding and science) can improve each other's performance. The instruction following domain can also improve the performance of these reasoning domains. All the reasoning domains and instruction following domain can not improve the performance in agent tasks, which means the systematicity of formal logic can not naturally translate into the pragmatic sequences required for tool manipulation, but the domain interference is still not observed. Thirdly, the comparison among different model merging methods is shown in Table 4, where the best results are in bold. The multi-teacher on-policy distillation is as effective as the direct weight merging methods, but it requires additional GPU hours. Different model

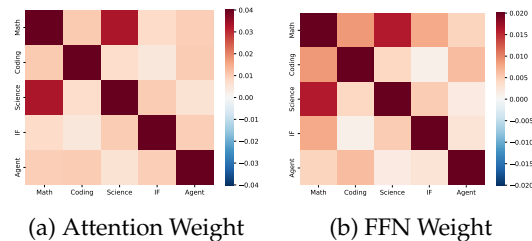


Figure 3: The cross-domain cosine similarity of weight shift vectors in the overlapping regions. We report the average scores on attention weights (Q, K, V and O) and FFN weights (FFN-up, FFN-down and FFN-gate).

merging methods exhibit a seesaw effect on multiple benchmarks, and we choose the best merging method with the average scores. Direct weight merging not only preserves the most performance of the different domains, but can even achieve further improvements, such as in AIME’24, AIME’25, HLE, IFEval and BFCL v3. This further verifies the gain effect between different domains from the weight perspective. Note that our best model using open source dataset achieves comparable performance with official Qwen3-4B model (Thinking mode) (Yang et al., 2025) as shown in Table 8, which verifies the effectiveness of our implementation.

3.3 Explore Weight Shift

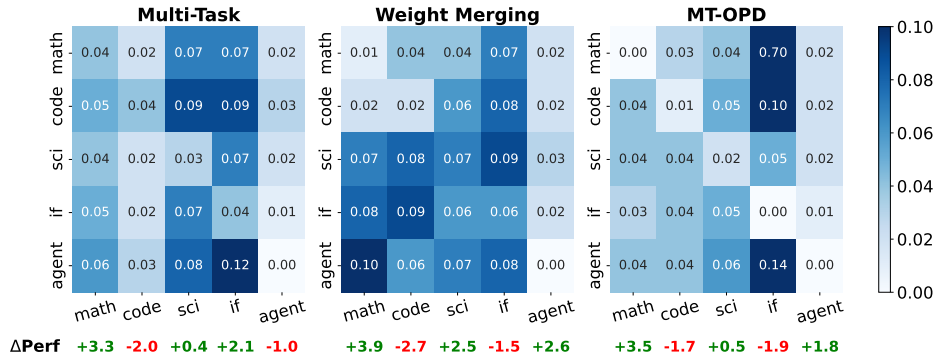
To ensure the robustness of the observed cross-domain gains, we evaluate the accuracy change trajectory throughout the reinforcement learning process of each individual domain. We select the benchmarks from various domains for credibility. Concretely, we choose AIME’24, LiveCodeBench v5, GPQA-Diamond, IFEval and BFCL v3 for math, coding, science, instruction following and agent respectively, and the results are shown in Figure 2. The reinforcement learning of three reasoning domains (i.e., math, coding and science) can stably improve each other’s performance. The instruction following domain can help in the evaluation of the three reasoning domains, whereas the inverse enhancement remains marginal. The reasoning domains and instruction following domain maintains the performance that fluctuates around the initial model in agent task. We further examine the weight shift of individual domain-specific RLVR models relative to the initial supervised fine-tuned model. Considering the impact of numerical precision of *bfloat16*, we consider a weight $w \in \mathbb{R}$ as changed when $|w_{RL} - w_{SFT}| > \eta \max(|w_{RL}|, |w_{SFT}|)$, $\eta = 1e^{-3}$. We can obtain the weight changed mask of each RLVR model $M_{RL} \in \{0, 1\}^d$ with d as the dimension of weights, and then calculate the Jaccard overlap $J(RL_1, RL_2) = \frac{|M_{RL_1} \wedge M_{RL_2}|}{|M_{RL_1} \vee M_{RL_2}|}$. We choose the representative weights in the 17-th layers following (Zhu et al., 2025). We find that the magnitude of weight updates represents an average of roughly 30% relative to the total number of weights, so we calculate the Jaccard overlap between two random mask $M_1 \in \{0, 1\}^d$ and $M_2 \in \{0, 1\}^d$ as reference, and their elements have a 30% probability of being 1. The cross-domain Jaccard overlap of weight changed masks is provided in Table 5. The weight update footprints in reinforcement learning across different domains have significant overlap. We then examine the cross-domain cosine similarity of the weight shift vectors in the overlapping regions to further assess their mutual influence. Considering that cosine similarity could encounter the curse of dimensionality in high-dimensional spaces, we use orthogonal random projection from Locality Sensitive Hashing (LSH). Concretely, we use a random orthogonal matrix to map all weight shift vectors to 256-dimension subspace and then calculate their cosine similarity. The results are shown in Figure 3 and the average scores on attention weights (Q, K, V and O) and FFN weights (FFN-up, FFN-down and FFN-gate) are reported. The cross-domain cosine similarity remains positive albeit at a modest level. Specifically, the three reasoning domains demonstrate higher mutual similarity to each other compared to that with the instruction following and agent domain.

3.4 Explore Policy Neighborhoods

Kullback-Leibler (KL) Divergence is commonly used to quantify the discrepancy between two probability distributions. In this work, we primarily consider the forward KL divergence, $KL(\pi_{old} \parallel \pi_{new})$. Prior work has shown that post-training procedures such as SFT and RL often lead to degradation on previously learned tasks as the KL divergence between the base model and the updated policy increases (Shenfeld et al., 2025). However, we observe no significant correlation between the KL divergence and the performance change during model merging or multi-task training. Despite model merging leads to an increased KL divergence with domain experts, domain performance shows inconsistent trends, suggesting that inter-domain interference is not absolute. Thus, exploring new metrics is essential in multi-domain scenarios.

Table 5: Cross-domain Jaccard overlap of weight changed masks for different weights in the 17-th layers. The Jaccard overlap between random masks is also provided as reference.

Domains	Q	K	V	O	FFN-dn	FFN-up	FFN-gt
Math - Coding	0.47	0.48	0.47	0.48	0.47	0.46	0.46
Math - Science	0.46	0.47	0.46	0.46	0.45	0.45	0.45
Math - IF	0.47	0.48	0.47	0.48	0.47	0.46	0.46
Math - Agent	0.47	0.48	0.47	0.48	0.47	0.46	0.46
Coding - Science	0.46	0.47	0.46	0.46	0.45	0.45	0.45
Coding - IF	0.47	0.48	0.47	0.48	0.47	0.46	0.46
Coding - Agent	0.47	0.48	0.48	0.48	0.47	0.46	0.47
Science - IF	0.46	0.47	0.46	0.46	0.45	0.45	0.45
Science - Agent	0.46	0.47	0.46	0.46	0.45	0.45	0.45
IF - Agent	0.47	0.48	0.47	0.48	0.47	0.46	0.46
random	0.18	0.18	0.18	0.18	0.18	0.18	0.18

Figure 4: Cross-comparison of KL divergence. The y-axis represents the domain of the expert model, while the x-axis indicates the data domain from which trajectories were sampled to compute the KL divergence. Each cell value represents the KL divergence. ΔPerf represents the performance change of the multi-domain model relative to the domain expert on the sampled domains.

To clearly investigate the causes of performance variations in multi-domain scenarios, it is necessary to decouple the effects of different domains. We cross-compare the KL divergence of different domain experts (i.e., π_{old}) with multi-domain policy models (i.e., π_{new}) across each domain, as shown in Figure 4. We find that, for a given test domain, experts from other domains can also exhibit relatively low KL divergence with the resulting multi-domain policy model. For example, when evaluating on *math* domain, the *math* expert exhibits the lowest KL divergence with the multi-task trained policy model, which is expected. Remarkably, the *coding* expert also shows a relatively low KL divergence, and the combined model achieves further performance gains in the *math* domain. These observations imply that, in multi-domain merging, policy distributions from various domains may interact with one another, especially for domain experts whose policies are close to the merged model.

Given a domain \mathcal{A} and its expert model $E_{\mathcal{A}}$, we define domain \mathcal{B} as a **policy neighborhood** of \mathcal{A} if the following condition is satisfied:

$$\mathbb{E}_{x \sim \mathcal{A}, \hat{y} \sim \pi_{E_{\mathcal{B}}}(\cdot | x)} \left[\log \frac{\pi_{E_{\mathcal{B}}}(\hat{y} | x)}{\pi_{\text{multi}}(\hat{y} | x)} \right] < \varepsilon, \quad (1)$$

where π_{multi} is the merged model policy and ε is a threshold that should be determined by comparing with KL ($\pi_{E_{\mathcal{A}}} \parallel \pi_{\text{multi}}$). Based on this definition, policy neighborhoods can be identified from Figure 4, where domain \mathcal{A} and \mathcal{B} can be selected at the x-axis and y-axis,

Table 6: Performance of models merged from different domain expert combinations using Ties merging. The policy neighborhoods can be identified from Figure 4: *coding* is a neighbor of *math* in *math* domain, and *agent* is a neighbor of *coding* in *coding* domain.

Domain(s)	AIME24	AIME25	Domain(s)	LCB v5	LCB v6
Math	77.66	70.42	Coding	65.00	58.86
Math + Coding	80.29 \uparrow 2.63	72.44 \uparrow 2.02	Coding + Math	60.42 \downarrow 4.58	57.17 \downarrow 1.69
Math + Science	75.07 \downarrow 2.59	67.65 \downarrow 2.77	Coding + Science	63.84 \downarrow 1.16	60.00 \uparrow 1.14
Math + IF	78.11 \uparrow 0.45	69.04 \downarrow 1.38	Coding + IF	59.30 \downarrow 5.70	59.43 \uparrow 0.57
Math + Agent	72.94 \downarrow 4.72	63.31 \downarrow 7.11	Coding + Agent	66.49 \uparrow 1.49	62.86 \uparrow 4.00

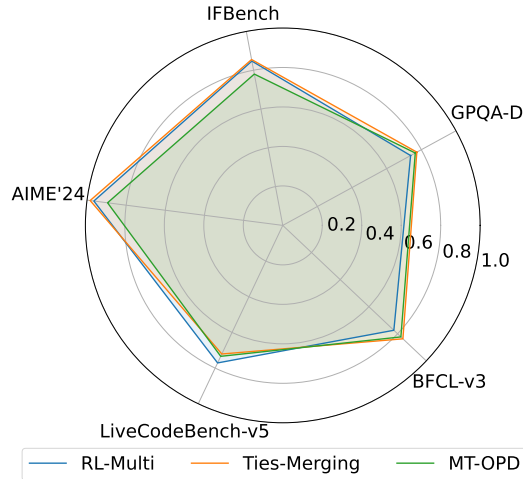


Figure 5: Accuracy gain consistency with union of single-task models on 5 benchmarks.

respectively. To further verify whether multi-domain methods benefit from neighboring policies, we conduct an ablation study on the domain combinations used for model merging, as shown in Table 6. We find that, for a given domain, merging with the domain expert’s neighboring policy experts further improves the domain performance. In contrast, merging non-neighboring policies does not necessarily yield extra gains. This shows that policy neighborhoods may be one of the factors enabling multi-domain merging to maintain or even enhance the performance of individual domains. Furthermore, we observe that the policy neighborhood relationship is asymmetric. For instance, in *math* domain, the *coding* expert is a neighboring policy for the *math* expert, but not vice versa in *coding* domain. This might be attributed to the inherent asymmetry of the KL divergence.

3.5 Do Multi-Task Learners and Merged Models Acquire the Same Skills as Single-Task Models?

The preceding experiments demonstrate that both multi-task training and model merging effectively develop expertise across multiple domains. A natural question arises: **do these multi-domain models acquire the same skills as their single-task counterparts?** To investigate this, we analyze the overlap of newly solved instances (relative to the SFT baseline) between multi-domain models and the collection of five single-task models. Specifically, for each task t , we define a gain vector $g_m^t = (\max(a_m^t(1) - a_{\text{sft}}^t(1), 0), \dots, \max(a_m^t(n_t) - a_{\text{sft}}^t(n_t), 0))$, where m denotes the model, n_t is the size of task t ’s test set, and $a_m^t(i)$ represents the accuracy of model m on the i -th the sample of task t . We then construct a union gain vector $g_{\text{union}}^t = \max(g_{\text{math}}^t, g_{\text{science}}^t, g_{\text{coding}}^t, g_{\text{IF}}^t, g_{\text{agent}}^t)$ to serve as a proxy for the collective skills acquired during the learning of a single-task. Finally, we compute the cosine similarity

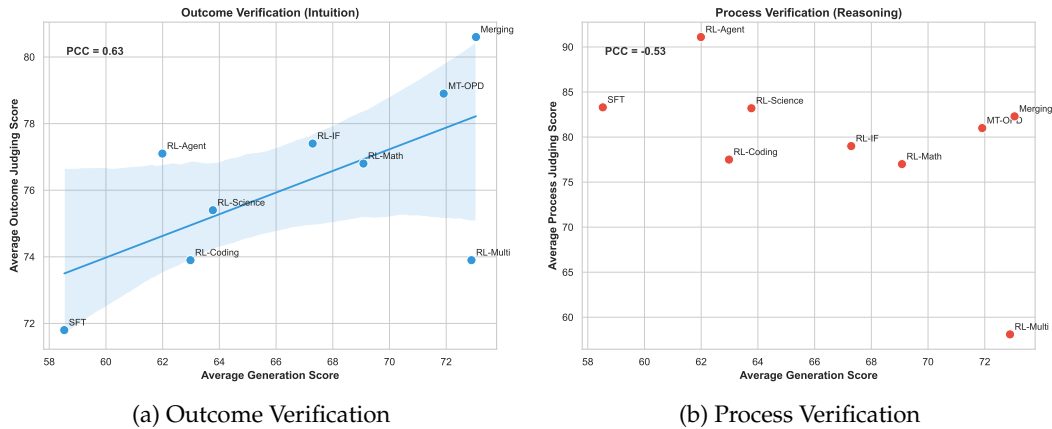


Figure 6: Correlation between average generation performance and average judge ability. Higher generation quality correlates with stronger self-judgment.

between g_{union}^f and the gain vectors of RL-Multi, Ties-Merging, and MT-OPD, respectively, as the measure of gain consistency. A higher similarity score indicates that a model inherits a greater proportion of skills originally developed through single-task learning.

As illustrated in Figure 5, all three models exhibit significant overlap with single-task models in their learned capabilities. Among the 5 benchmarks, the math task shows the highest consistency in performance gains, suggesting that mathematical skills may be more homogeneous (inherent) and resistant to inter-task interference. In contrast, for other domains, all three models appear to develop distinct proficiencies that are not captured during single-task learning.

In a cross-method comparison, the gain consistency of the model parameter merging method (Ties-Merging) is significantly higher than that of RL-Multi and MT-OPD on most domains. This observation provides an insight: **Model parameter merging primarily inherits the original capabilities of the single-task models, whereas the capabilities learned through multi-task training and on-policy distillation exhibit a larger divergence from those learned via single-task training**, which confirms the existence of emergent capabilities in multi-task models, which arise from tasks mutually promoting each other during learning. Given that the performance of multi-task models is not always superior to single-task models, it further indicates the simultaneous presence of inter-task interference phenomena.

3.6 The Dynamics of Self-Verification

In this section, we evaluate our RL-trained models as Generative Reward Models (GenRMs) operating on their own trajectories. We contrast two verification modalities: outcome-based verification, where the verifier observes only the final answer (approximating intuition), and process-based verification, where the verifier observes the full Chain-of-Thought (approximating reasoning). Across all models, we observe a positive correlation between average generation performance and outcome-based judge ability. Conversely, process-based judge ability exhibits a negative correlation (i.e., Pearson Correlation Coefficient (PCC) $r = -0.53$) with overall generation score, revealing more complex dynamics depending on the task structure and training methods, as shown in Figure 6. This indicates that while intuitive, outcome-level self-discrimination emerges naturally alongside generation improvements, rigorous process-level verification can actually degrade as models over-optimize for task-specific generation during extended reinforcement learning.

Finding 1: task structure dictates the verification modality. The effectiveness of a verification modality is heavily dependent on the inherent structure of the task domain. For logic-intensive tasks such as Mathematics (AIME), Coding (LCB), and Science (GPQA), process-based verification consistently outperforms outcome-based verification. In these

Table 7: Model performance on generation and self-critic evaluation tasks. “Gen” denotes generation benchmark scores. “Judge (Out/Proc)” denotes self-critic evaluation scores (Avg@8 × 100) where “Out” denotes outcome judging (content mode) and “Proc” denotes process judging (reasoning mode). Higher is better for all metrics.

Model	AIME24 (Math)		IFEval (Inst)		LCB v5 (Code)		GPQA (Science)		Avg	
	Gen	Judge (Out/Proc)	Gen	Judge (Out/Proc)	Gen	Judge (Out/Proc)	Gen	Judge (Out/Proc)	Gen	Judge (Out/Proc)
SFT	56.04	72.9 / 91.8	79.48	81.6 / 72.3	55.92	84.4 / 95.7	42.68	48.3 / 73.4	58.53	71.8 / 83.3
RL-Math	77.66	81.2 / 93.8	80.59	77.8 / 64.2	59.59	87.2 / 93.7	58.46	60.9 / 56.2	69.08	76.8 / 77.0
RL-Coding	61.61	75.8 / 82.9	78.74	81.0 / 65.5	65.00	87.5 / 94.2	46.59	51.2 / 67.5	62.98	73.9 / 77.5
RL-Science	64.69	67.1 / 86.2	78.93	84.6 / 71.0	57.66	<u>90.9 / 97.1</u>	53.79	59.1 / <u>78.5</u>	63.77	75.4 / 83.2
RL-IF	67.81	83.8 / 90.4	90.94	87.4 / 61.6	60.80	82.4 / 91.6	49.62	56.0 / 72.3	67.29	77.4 / 79.0
RL-Agent	57.60	76.7 / 95.3	81.33	85.1 / 88.5	62.95	91.6 / 99.4	46.09	55.1 / 81.1	61.99	77.1 / 91.1
Merging	<u>81.15</u>	82.9 / 93.3	<u>92.61</u>	<u>91.0 / 79.1</u>	60.84	88.4 / 95.8	<u>57.58</u>	<u>59.9</u> / 61.1	73.05	80.6 / 82.3
RL-Multi	81.20	86.7 / 86.2	93.53	80.5 / 27.5	63.21	72.3 / 76.1	53.62	55.9 / 42.6	<u>72.89</u>	73.9 / 58.1
MT-OPD	80.52	<u>85.8</u> / 91.2	90.20	<u>87.5</u> / 66.5	<u>63.26</u>	85.0 / 94.7	53.66	57.1 / 71.4	71.91	<u>78.9</u> / 81.0

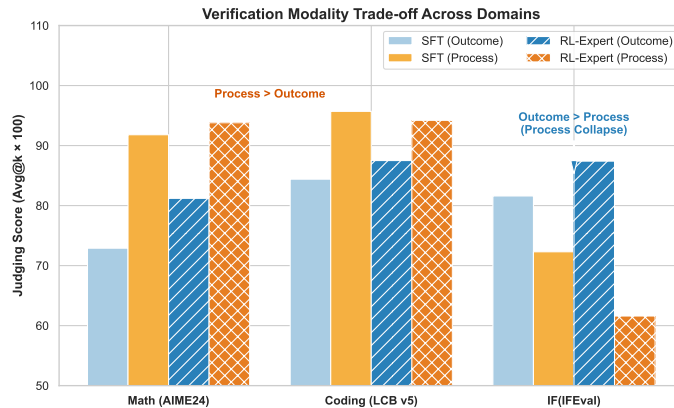


Figure 7: Verification modality trade-off across domains. For reasoning tasks (Math/Coding), process verification is superior because errors are hidden in the derivation. For constraint tasks (IFEval), outcome verification is superior because errors manifest in execution. Furthermore, domain-specific RL training sharpens these modalities accordingly.

domains, the final answer is a highly compressed representation of a complex derivation. Evaluating only the outcome forces the verifier to make uninformed estimations, whereas process verification enables the model to detect logical fractures step-by-step before they propagate to the final result. Conversely, for constraint-intensive tasks like instruction following (IFEval), process-based verification severely underperforms. In constraint satisfaction, errors typically manifest in surface-level execution, such as violating JSON syntax or length restrictions. When evaluating these tasks, the reasoning trace often merely states the model’s intent (e.g., “I will output exactly three bullet points”), while the final output reflects the actual execution. Relying on process verification here creates an intent-execution gap: the judge positively evaluates the correct plan within the reasoning trace, resulting in false positives that blind the model to actual formatting failures in the output.

Finding 2: the agentic advantage in process verification. We observe that the RL-Agent, optimized specifically for multi-turn general tool-use tasks, significantly outperforms other single-domain models in process-based verification. As demonstrated in Table 7, the RL-Agent achieves the highest process judging scores across diverse domains, including 95.3 on AIME, 88.5 on IFEval, and 99.4 on LCB. Unlike static mathematical derivations, agentic training involves state interactions where the model must continuously evaluate intermediate tool-call returns and environmental feedback. This multi-step optimization forces the model to verify its own trajectory dynamically. Consequently, the model develops a highly robust sequential monitoring capability. This indicates that interactive, multi-turn training is a critical catalyst for cultivating reliable process judges, effectively training the model to treat the reasoning traces as functional, verifiable logs.

Finding 3: scaling multi-task RL vs. expert integration (the robustness trade-off). While combining diverse training signals theoretically yields comprehensive models, scaling

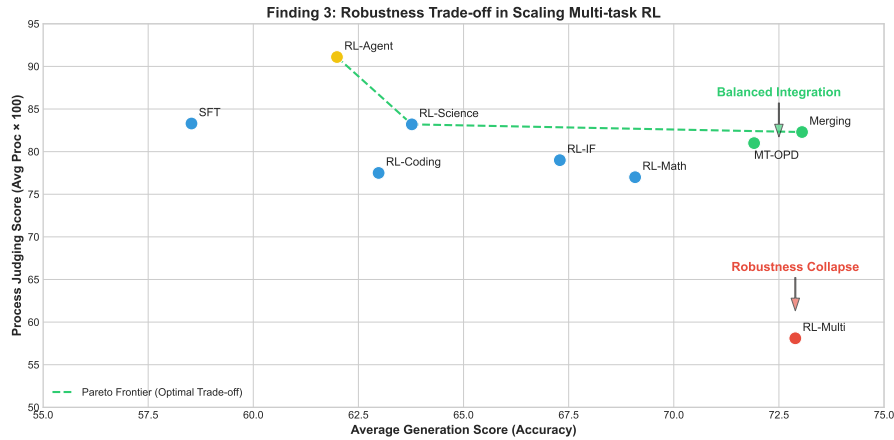


Figure 8: Robustness trade-off in scaling multi-task RL. Multi-task RL exhibits a severe collapse in process verification, whereas decoupled integration methods remain stable.

these multi-task approaches reveals a distinct robustness trade-off, as shown in Figure 8. Extended multi-task RL (RL-Multi) improves overall generation quality but induces a severe degradation in process verification capabilities. For instance, while RL-Multi achieves a competitive generation average of 72.89, its process verification score collapses to 27.5 on IFEval and 42.6 on GPQA. This instability suggests that competing gradient signals across heterogeneous domains eventually cause gradient interference; the model’s internal critic misaligns, optimizing for superficial text patterns rather than rigorous evaluation. In contrast, methods that decouple expert training before integration prove significantly more stable. Weight merging, which operates directly in the parameter space by averaging the weights of specialized models, achieves the highest average generation (73.05) and outcome judgment (80.6). This demonstrates that weight averaging acts as an effective regularizer, preserving general capabilities while filtering out the over-optimized noise inherent to extended RL runs. Meanwhile, MT-OPD (Multi-Teacher On-Policy Distillation) integrates expert knowledge in the behavior space. By utilizing multi-teacher supervisions on generated trajectories, MT-OPD prevents the model from overfitting to a single domain’s reasoning style, securing a robust and balanced foundation for both outcome and process verification.

4 Conclusion

In this work, we present a systematic study of multi-domain reinforcement learning, comparing the mixed multi-task training paradigm with separate domain-specific training followed by model merging. Our extensive experiments across math, coding, science, instruction following and agent reveal that multi-task RLVR exhibits minimal inter-task interference. Instead, reasoning-intensive domains demonstrate significant synergistic effects. Through in-depth analyses of weight shift footprints and policy KL divergence, we identify the underlying mechanisms of these gains: multi-task training facilitates neighborhood policy transfer that drives domain-specific policies toward a global optimum. These findings provide critical insights into the scalability and efficiency of developing general reasoning models, suggesting the collaborative potential of verifiable rewards across domains is a promising frontier for post-training of LLMs.

References

Rishabh Agarwal, Nino Vieillard, Yongchao Zhou, Piotr Stanczyk, Sabela Ramos Garea, Matthieu Geist, and Olivier Bachem. On-policy distillation of language models: Learning from self-generated mistakes. In *The twelfth international conference on learning representations*, 2024.

- AIME. AIME problems and solutions, 2025. URL https://artofproblemsolving.com/wiki/index.php/AIME_Problems_and_Solutions.
- Alon Albalak, Duy Phung, Nathan Lile, Rafael Rafailov, Kanishk Gandhi, Louis Castricato, Anikait Singh, Chase Blagden, Violet Xiang, Dakota Mahan, et al. Big-math: A large-scale, high-quality math dataset for reinforcement learning in language models. *arXiv preprint arXiv:2502.17387*, 2025.
- Fengshuo Bai, Hongming Zhang, Tianyang Tao, Zhiheng Wu, Yanna Wang, and Bo Xu. Picor: Multi-task deep reinforcement learning with policy correction. In *Proceedings of the AAAI Conference on Artificial Intelligence*, volume 37, pp. 6728–6736, 2023.
- Aaron Blakeman, Aaron Grattafiori, Aarti Basant, Abhibha Gupta, Abhinav Khattar, Adi Renduchintala, Aditya Vavre, Akanksha Shukla, Akhiad Bercovich, Aleksander Ficek, et al. Nemotron 3 nano: Open, efficient mixture-of-experts hybrid mamba-transformer model for agentic reasoning. *arXiv preprint arXiv:2512.20848*, 2025.
- Bytedance-Seed-Foundation-Code-Team, :, Yao Cheng, Jianfeng Chen, Jie Chen, Li Chen, Liyu Chen, Wentao Chen, Zhengyu Chen, Shijie Geng, Aoyan Li, Bo Li, Bowen Li, Linyi Li, Boyi Liu, Jiaheng Liu, Kaibo Liu, Qi Liu, Shukai Liu, Siyao Liu, Tianyi Liu, Tingkai Liu, Yongfei Liu, Rui Long, Jing Mai, Guanghan Ning, Z. Y. Peng, Kai Shen, Jiahao Su, Jing Su, Tao Sun, Yifan Sun, Yunzhe Tao, Guoyin Wang, Siwei Wang, Xuwu Wang, Yite Wang, Zihan Wang, Jinxiang Xia, Liang Xiang, Xia Xiao, Yongsheng Xiao, Chenguang Xi, Shulin Xin, Jingjing Xu, Shikun Xu, Hongxia Yang, Jack Yang, Yingxiang Yang, Jianbo Yuan, Jun Zhang, Yufeng Zhang, Yuyu Zhang, Shen Zheng, He Zhu, and Ming Zhu. Fullstack bench: Evaluating llms as full stack coders, 2025. URL <https://arxiv.org/abs/2412.00535>.
- Yongchao Chen, Yueying Liu, Junwei Zhou, Yilun Hao, Jingquan Wang, Yang Zhang, and Chuchu Fan. R1-code-interpreter: Training llms to reason with code via supervised and reinforcement learning. *arXiv preprint arXiv:2505.21668*, 2025.
- Ganqu Cui, Lifan Yuan, Zefan Wang, Hanbin Wang, Yuchen Zhang, Jiacheng Chen, Wendi Li, Bingxiang He, Yuchen Fan, Tianyu Yu, et al. Process reinforcement through implicit rewards. *arXiv preprint arXiv:2502.01456*, 2025.
- Guanting Dong, Hangyu Mao, Kai Ma, Licheng Bao, Yifei Chen, Zhongyuan Wang, Zhongxia Chen, Jiazhen Du, Huiyang Wang, Fuzheng Zhang, et al. Agentic reinforced policy optimization. *arXiv preprint arXiv:2507.19849*, 2025.
- Chang Gao, Chuji Zheng, Xiong-Hui Chen, Kai Dang, Shixuan Liu, Bowen Yu, An Yang, Shuai Bai, Jingren Zhou, and Junyang Lin. Soft adaptive policy optimization. *arXiv preprint arXiv:2511.20347*, 2025.
- Daya Guo, Dejian Yang, Haowei Zhang, Junxiao Song, Ruoyu Zhang, Runxin Xu, Qihao Zhu, Shirong Ma, Peiyi Wang, Xiao Bi, et al. Deepseek-r1: Incentivizing reasoning capability in llms via reinforcement learning. *arXiv preprint arXiv:2501.12948*, 2025.
- Jujie He, Jiakai Liu, Chris Yuhao Liu, Rui Yan, Chaojie Wang, Peng Cheng, Xiaoyu Zhang, Fuxiang Zhang, Jiacheng Xu, Wei Shen, Siyuan Li, Liang Zeng, Tianwen Wei, Cheng Cheng, Bo An, Yang Liu, and Yahui Zhou. Skywork open reasoner 1 technical report. *arXiv preprint arXiv:2505.22312*, 2025a.
- Jujie He, Jiakai Liu, Chris Yuhao Liu, Rui Yan, Chaojie Wang, Peng Cheng, Xiaoyu Zhang, Fuxiang Zhang, Jiacheng Xu, Wei Shen, Siyuan Li, Liang Zeng, Tianwen Wei, Cheng Cheng, Yang Liu, and Yahui Zhou. Skywork open reasoner series, 2025b. Notion Blog.
- Oğuz Kağan Hitit, Leander Girkbach, and Zeynep Akata. A systematic study of model merging techniques in large language models. *arXiv preprint arXiv:2511.21437*, 2025.
- Binyuan Hui, Jian Yang, Zeyu Cui, Jiayi Yang, Dayiheng Liu, Lei Zhang, Tianyu Liu, Jiajun Zhang, Bowen Yu, Keming Lu, et al. Qwen2. 5-coder technical report. *arXiv preprint arXiv:2409.12186*, 2024.

- Gabriel Ilharco, Marco Tulio Ribeiro, Mitchell Wortsman, Suchin Gururangan, Ludwig Schmidt, Hannaneh Hajishirzi, and Ali Farhadi. Editing models with task arithmetic. *arXiv preprint arXiv:2212.04089*, 2022.
- Aaron Jaech, Adam Kalai, Adam Lerer, Adam Richardson, Ahmed El-Kishky, Aiden Low, Alec Helyar, Aleksander Madry, Alex Beutel, Alex Carney, et al. Openai o1 system card. *arXiv preprint arXiv:2412.16720*, 2024.
- Naman Jain, King Han, Alex Gu, Wen-Ding Li, Fanjia Yan, Tianjun Zhang, Sida Wang, Armando Solar-Lezama, Koushik Sen, and Ion Stoica. Livecodebench: Holistic and contamination free evaluation of large language models for code. *arXiv preprint arXiv:2403.07974*, 2024.
- Diederik P Kingma. Adam: A method for stochastic optimization. *arXiv preprint arXiv:1412.6980*, 2014.
- Nathan Lambert, Jacob Morrison, Valentina Pyatkin, Shengyi Huang, Hamish Ivison, Faeze Brahman, Lester James V Miranda, Alisa Liu, Nouha Dziri, Shane Lyu, et al. Tulu 3: Pushing frontiers in open language model post-training. *arXiv preprint arXiv:2411.15124*, 2024.
- Yujia Li, David Choi, Junyoung Chung, Nate Kushman, Julian Schrittwieser, Rémi Leblond, Tom Eccles, James Keeling, Felix Gimeno, Agustin Dal Lago, Thomas Hubert, Peter Choy, Cyprien de Masson d’Autume, Igor Babuschkin, Xinyun Chen, Po-Sen Huang, Johannes Welbl, Sven Gowal, Alexey Cherepanov, James Molloy, Daniel Mankowitz, Esme Sutherland Robson, Pushmeet Kohli, Nando de Freitas, Koray Kavukcuoglu, and Oriol Vinyals. Competition-level code generation with alphacode. *arXiv preprint arXiv:2203.07814*, 2022.
- MAA. American invitational mathematics examination-aime 2024, 2024, 2024.
- Michael S Matena and Colin A Raffel. Merging models with fisher-weighted averaging. *Advances in Neural Information Processing Systems*, 35:17703–17716, 2022.
- NVIDIA. Nemo gym: An open source library for scaling reinforcement learning environments for llm. <https://github.com/NVIDIA-NeMo/Gym>, 2025. GitHub repository.
- NVIDIA Corporation. Opensciencereasoning-2 dataset. Hugging Face Dataset, 2025. Available at: <https://huggingface.co/datasets/nvidia/OpenScienceReasoning-2>.
- Guilherme Penedo, Anton Lozhkov, Hynek Kydlíček, Loubna Ben Allal, Edward Beeching, Agustín Piqueres Lajarín, Quentin Gallouédec, Nathan Habib, Lewis Tunstall, and Leandro von Werra. Codeforces. <https://huggingface.co/datasets/open-r1/codeforces>, 2025.
- Long Phan, Alice Gatti, Ziwen Han, Nathaniel Li, Josephina Hu, Hugh Zhang, Chen Bo Calvin Zhang, Mohamed Shaaban, John Ling, Sean Shi, et al. Humanity’s last exam. *arXiv preprint arXiv:2501.14249*, 2025.
- Valentina Pyatkin, Saumya Malik, Victoria Graf, Hamish Ivison, Shengyi Huang, Pradeep Dasigi, Nathan Lambert, and Hannaneh Hajishirzi. Generalizing verifiable instruction following. *arXiv preprint arXiv:2507.02833*, 2025.
- Qwen Team. Qwq-32b: Embracing the power of reinforcement learning, March 2025. URL <https://qwenlm.github.io/blog/qwq-32b/>.
- David Rein, Betty Li Hou, Asa Cooper Stickland, Jackson Petty, Richard Yuanzhe Pang, Julien Dirani, Julian Michael, and Samuel R Bowman. Gpqa: A graduate-level google-proof q&a benchmark. In *First Conference on Language Modeling*, 2024.
- Zhihong Shao, Peiyi Wang, Qihao Zhu, Runxin Xu, Junxiao Song, Xiao Bi, Haowei Zhang, Mingchuan Zhang, YK Li, Yang Wu, et al. Deepseekmath: Pushing the limits of mathematical reasoning in open language models. *arXiv preprint arXiv:2402.03300*, 2024.

- Idan Shenfeld, Jyothish Pari, and Pulkit Agrawal. RL’s razor: Why online reinforcement learning forgets less. *arXiv preprint arXiv:2509.04259*, 2025.
- Fanqi Wan, Longguang Zhong, Ziyi Yang, Ruijun Chen, and Xiaojun Quan. Fusechat: Knowledge fusion of chat models. In *Proceedings of the 2025 Conference on Empirical Methods in Natural Language Processing*, pp. 21629–21653, 2025.
- Xumeng Wen, Zihan Liu, Shun Zheng, Shengyu Ye, Zhirong Wu, Yang Wang, Zhijian Xu, Xiao Liang, Junjie Li, Ziming Miao, et al. Reinforcement learning with verifiable rewards implicitly incentivizes correct reasoning in base llms. *arXiv preprint arXiv:2506.14245*, 2025.
- Mitchell Wortsman, Gabriel Ilharco, Samir Ya Gadre, Rebecca Roelofs, Raphael Gontijo-Lopes, Ari S Morcos, Hongseok Namkoong, Ali Farhadi, Yair Carmon, Simon Kornblith, et al. Model soups: averaging weights of multiple fine-tuned models improves accuracy without increasing inference time. In *International conference on machine learning*, pp. 23965–23998. PMLR, 2022.
- Runzhe Wu, Ankur Samanta, Ayush Jain, Scott Fujimoto, Jeongyeol Kwon, Ben Kretzu, Youliang Yu, Kaveh Hassani, Boris Vidolov, and Yonathan Efroni. Imbalanced gradients in rl post-training of multi-task llms. *arXiv preprint arXiv:2510.19178*, 2025.
- Bangjun Xiao, Bingquan Xia, Bo Yang, Bofei Gao, Bowen Shen, Chen Zhang, Chenhong He, Chiheng Lou, Fuli Luo, Gang Wang, et al. Mimo-v2-flash technical report. *arXiv preprint arXiv:2601.02780*, 2026.
- Prateek Yadav, Derek Tam, Leshem Choshen, Colin Raffel, and Mohit Bansal. Resolving interference when merging models. *arXiv preprint arXiv:2306.01708*, 1, 2023a.
- Prateek Yadav, Derek Tam, Leshem Choshen, Colin A Raffel, and Mohit Bansal. Ties-merging: Resolving interference when merging models. *Advances in Neural Information Processing Systems*, 36:7093–7115, 2023b.
- Fanjia Yan, Huanzhi Mao, Charlie Cheng-Jie Ji, Tianjun Zhang, Shishir G. Patil, Ion Stoica, and Joseph E. Gonzalez. Berkeley function calling leaderboard. https://gorilla.cs.berkeley.edu/blogs/8_berkeley_function_calling_leaderboard.html, 2024.
- An Yang, Beichen Zhang, Binyuan Hui, Bofei Gao, Bowen Yu, Chengpeng Li, Dayiheng Liu, Jianhong Tu, Jingren Zhou, Junyang Lin, et al. Qwen2. 5-math technical report: Toward mathematical expert model via self-improvement. *arXiv preprint arXiv:2409.12122*, 2024.
- An Yang, Anfeng Li, Baosong Yang, Beichen Zhang, Binyuan Hui, Bo Zheng, Bowen Yu, Chang Gao, Chengen Huang, Chenxu Lv, et al. Qwen3 technical report. *arXiv preprint arXiv:2505.09388*, 2025.
- Le Yu, Bowen Yu, Haiyang Yu, Fei Huang, and Yongbin Li. Language models are super mario: Absorbing abilities from homologous models as a free lunch. In *Forty-first International Conference on Machine Learning*, 2024.
- Qiyang Yu, Zheng Zhang, Ruofei Zhu, Yufeng Yuan, Xiaochen Zuo, Yu Yue, Weinan Dai, Tiantian Fan, Gaohong Liu, Lingjun Liu, et al. Dapo: An open-source llm reinforcement learning system at scale. *arXiv preprint arXiv:2503.14476*, 2025.
- Tianhe Yu, Saurabh Kumar, Abhishek Gupta, Sergey Levine, Karol Hausman, and Chelsea Finn. Gradient surgery for multi-task learning. *Advances in neural information processing systems*, 33:5824–5836, 2020.
- Yang Yue, Zhiqi Chen, Rui Lu, Andrew Zhao, Zhaokai Wang, Shiji Song, and Gao Huang. Does reinforcement learning really incentivize reasoning capacity in llms beyond the base model? *arXiv preprint arXiv:2504.13837*, 2025.
- Aohan Zeng, Xin Lv, Qinkai Zheng, Zhenyu Hou, Bin Chen, Chengxing Xie, Cunxiang Wang, Da Yin, Hao Zeng, Jiajie Zhang, et al. Glm-4.5: Agentic, reasoning, and coding (arc) foundation models. *arXiv preprint arXiv:2508.06471*, 2025.

Kaiyan Zhang, Yuxin Zuo, Bingxiang He, Youbang Sun, Runze Liu, Che Jiang, Yuchen Fan, Kai Tian, Guoli Jia, Pengfei Li, et al. A survey of reinforcement learning for large reasoning models. *arXiv preprint arXiv:2509.08827*, 2025.

Wenting Zhao, Xiang Ren, Jack Hessel, Claire Cardie, Yejin Choi, and Yuntian Deng. Wildchat: 1m chatgpt interaction logs in the wild. *arXiv preprint arXiv:2405.01470*, 2024.

Chujie Zheng, Shixuan Liu, Mingze Li, Xiong-Hui Chen, Bowen Yu, Chang Gao, Kai Dang, Yuqiong Liu, Rui Men, An Yang, et al. Group sequence policy optimization. *arXiv preprint arXiv:2507.18071*, 2025.

Jeffrey Zhou, Tianjian Lu, Swaroop Mishra, Siddhartha Brahma, Sujoy Basu, Yi Luan, Denny Zhou, and Le Hou. Instruction-following evaluation for large language models. *CoRR*, abs/2311.07911, 2023.

Hanqing Zhu, Zhenyu Zhang, Hanxian Huang, DiJia Su, Zechun Liu, Jiawei Zhao, Igor Fedorov, Hamed Pirsiavash, Zhizhou Sha, Jinwon Lee, et al. The path not taken: RLvr provably learns off the principals. *arXiv preprint arXiv:2511.08567*, 2025.

Qihao Zhu, Daya Guo, Zhihong Shao, Dejian Yang, Peiyi Wang, Runxin Xu, Y Wu, Yukun Li, Huazuo Gao, Shirong Ma, et al. Deepseek-coder-v2: Breaking the barrier of closed-source models in code intelligence. *arXiv preprint arXiv:2406.11931*, 2024.

Table 8: Comparison between the official Qwen3-4B model (Thinking mode) from (Yang et al., 2025) and our post-training implementation using open source dataset.

Methods	AIME'24	AIME'25	LCB v5	LCB v6	HLE	GPQA-D	IFEval	IFBench	BFCL v3	Avg.
Qwen3-4B (Thinking)	73.80	65.60	54.20	46.86	4.73	55.90	81.90	27.55	65.90	52.94
Our (open source data)	81.15	74.74	60.84	57.71	7.92	57.58	92.61	54.76	61.73	61.00

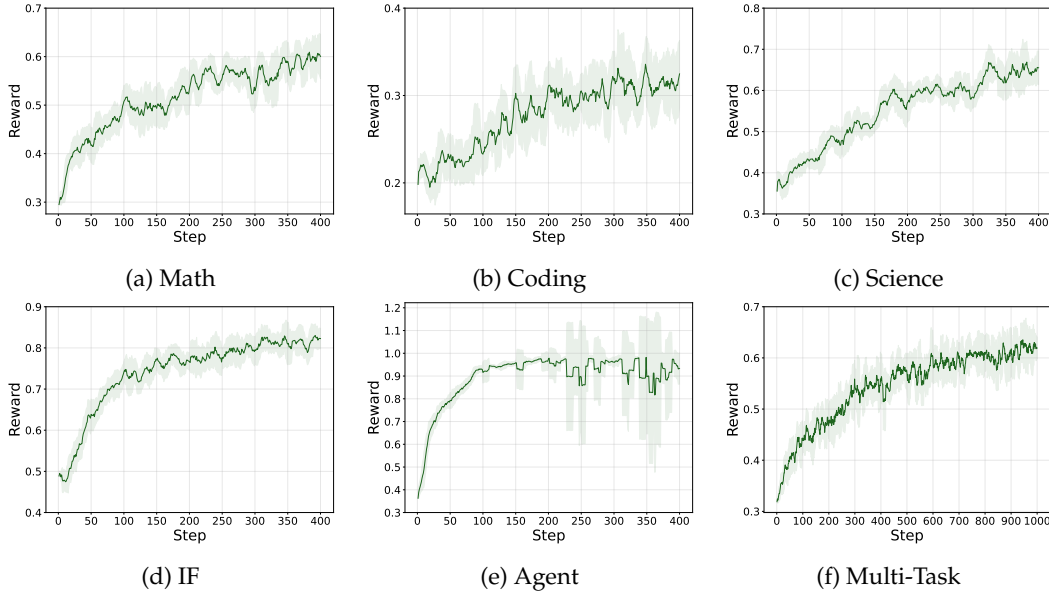


Figure 9: The trajectories of training rewards in five domain-specific RLVR training and multi-task RLVR training.

A More Training details

Supervised fine-tuning. We use the Adam (Kingma, 2014) optimizer with the learning rate of $5e^{-5}$ and weight decay of 0.1, and the 10% training steps are used for learning rate warmup. We set the the batch size of 512 with average response length of 7K.

Reinforcement learning. For single-domain reinforcement learning, we use GRPO with a group size of 16 and enable masked importance sampling to ensure consistency between training and inference. We use a batch size of 128 and perform one gradient update per 2048 rollouts. The maximum generation length is set to 32k tokens, and we use a sampling temperature of 1.0 to promote exploration. Each domain is trained for 400 steps with a constant learning rate of 2×10^{-6} . For the math answer verification, we adopt the evaluator from Qwen QwQ-32B (Qwen Team, 2025). For the instruction following evaluation, we use the IFEvalG verifier (Lambert et al., 2024). For the coding evaluation, we employ SandboxFusion (Bytedance-Seed-Foundation-Code-Team et al., 2025) as the execution sandbox to obtain unit test results. For the agent training, we use NVIDIA NeMo-Gym (NVIDIA, 2025) to provide an interactive environments. In the other hand, for the multi-task reinforcement learning, we apply the domain-routed reward function. Concretely, each batch contains a random mixture of data from different domains and each kind of task can receive corresponding rollouts for estimating the gradient direction. The training setting is basically the same with the single-domain reinforcement learning, except that we train 1000 steps for multi-task training. All reinforcement learning training tasks use Adam optimizer with the weight decay of 0.1. We conduct all RLVR training on the same kind of GPUs with *slime*³ framework, and the corresponding GPU hours are provided in Table 2. The trajectories of training rewards are provided in Figure 9.

³<https://github.com/THUDM/slime>

Multi-teacher on-policy distillation. We conduct multi-teacher on-policy distillation for 200 steps with the batch size of 256 and a group size of 4. The gradient update is conducted per 1024 rollouts. We use Adam optimizer with the learning rate of $1e^{-6}$.